Optimal Classifier for an ML-Assisted Resource Allocation in Wireless Communications

Rashika Raina, *Student Member, IEEE*, David E. Simmons, Nidhi Simmons, *Senior Member, IEEE*, and Michel Daoud Yacoub, *Member, IEEE*

***Abstract*—This letter advances on the outage probability (OP) performance of a machine learning (ML)-assisted single-user multi-resource system. We focus on OP optimality and the trade-off between outage improvement and the mean number of resources scanned until a suitable resource is captured. We first present expressions for the OP of this system, complemented by an outage loss function (OLF) for its minimization. We then derive: (i) the necessary and sufficient properties of an optimal model (OpM) and (ii) expressions for the average number of resources scanned by both OpM and non-OpMs. Here, non-OpMs refer to those trained with the OLF and binary cross entropy (BCE) loss functions. We establish that optimal performance requires a channel that exhibits no time decorrelation properties. For very high decorrelation values, we find that models trained using the OLF and BCE perform similarly. For intermediate (practical) decorrelation values, OLF outperforms BCE, and both approach the OpM as decorrelation tends to zero. Our analysis further reveals that, to be able to capture a suitable resource, models trained with the OLF scan a slightly higher number of resources than the OpM and those trained with BCE. This increase in the mean number of scanned resources is offset by a significant enhancement in the OP as compared to BCE.**

***Index Terms*—Machine learning, Outage prediction, Outage loss function, Optimal Classifier, Resource allocation.**

I. Introduction

Connectivity disruption in wireless communications is commonly associated with the inherent signal variability in the radio channels. Implementing techniques to combat this has long been the subject of intense research. As in many other areas, machine learning (ML) has emerged as a powerful tool with great potential to improve the performance of wireless systems. For instance, ML can be successfully used in forecasting quality-of-service degradation and enhancing the reliability of advanced wireless networks [1]. Additionally, beamforming vector observations, channel metrics, and geographical as well as visual information [2] can benefit from ML techniques to preemptively identify link blockages [3]. ML has also been used to enhance resource management in wireless networks. For example, deep learning and deep reinforcement learning were used to optimize power allocation in massive multiple-input multiple-output systems [4], and vehicle-to-vehicle communications [5], respectively.

This work was supported by the Royal Academy of Engineering (Grant ref RF\201920\19\191).

R. Raina and N. Simmons are with the Centre for Wireless Innovation, Queen's University of Belfast, Belfast, BT3 9DT, UK, (e-mail: {rraina01, nidhi.simmons}@qub.ac.uk). D.E. Simmons is with Dhali Holdings Ltd., Belfast BT5 7HW, UK, (e-mail: dr.desimmons@gmail.com). M. D. Yacoub is with the School of Electrical and Computer Engineering, University of Campinas, Campinas 13083-970, Brazil, (e-mail: mdyacoub@unicamp.br).

Despite advancements, most of these studies have focused on traditional loss functions like binary cross entropy (BCE) or mean squared error for training ML models, potentially limiting performance gains in future systems. In contrast, [6] underscored the benefits of incorporating domain-specific knowledge into ML models. Expanding on this, [7] employed an ML model with a custom loss function to optimize reflection coefficients of reconfigurable intelligent surfaces and [8] utilized it for resource allocation in beyond-5G network slicing. Furthermore, [9] developed a custom loss function, hereafter referred to as the outage loss function (OLF), to optimize ML model training in a resource allocation system with a focus on minimizing outage probabilities (OPs).

Our contribution builds on [9] by determining the necessary and sufficient properties of an optimal ML outage classifier. We demonstrate that optimal performance is achievable only when the model and the channel are perfectly correlated. Furthermore, as the correlation approaches one, the performance of the non-optimal models (non-OpMs) converges towards the optimal model (OpM). Here, non-OpMs are defined as those trained using the OLF and BCE. Following this, we quantify the average number of resources scanned by both the OpM and non-OpMs until a suitable resource can be captured. Our results suggest that models trained using OLF adopt a careful resource acceptance strategy, especially in scenarios characterized by infrequent outages and high signal-to-noise ratios (SNRs) than the OpM and those trained using BCE (assuming the same classification threshold). Consequently, on average, to capture a suitable resource, OLF models tend to scan slightly more resources, but with the benefit of a substantial reduction in the system's OP as compared to BCE.

II. System Model - Revisited

This work considers the system model from [9], and restates formulations relevant to our current analysis. The focus is on a single-user multi-resource system, where each resource $j \in \mathsf{R}$ is characterized by a variable channel state over time, $h_j(t) \in \mathbb{C}$. For any two distinct resources j and j', their channel states $h_j(t)$ and $h_{j'}(t)$ are independent and identically distributed (i.i.d.) for $j \neq j'$. Furthermore, the correlation between $h_j(t)$ and $h_j(t+l)$, where $l \in \mathbb{N}$, decreases as l increases, and approaches zero as $l \to \infty$. The user employs an ML model designed to learn these correlations, aiding in the selection of an appropriate resource (discussed in the next paragraph). Let $H_j(t, \mathtt{k}) \triangleq [h_j(t-\mathtt{k}+1), \cdots, h_j(t)]^T \in \mathbb{C}^{\mathtt{k}}$ be the sequence of historical channel state samples for resource j. The capacity

$C\left(H_j(t+l,l)\right) \in \mathbb{R}^+$ of resource j from time $t+1$ to $t+l$ determines its support for user communication. For a quasi-static Gaussian channel, this is given by [10, eq. (5.80)]:

$$C(H_j(t+l,l)) = \sum_{i=1}^{l} \log_2\left(1+\mathtt{SNR}\left|h_j\left(t+i\right)\right|^2\right) \text{ bits/s/Hz.} \quad (1)$$

Here, SNR represents the average SNR per sample. If the user's required communication rate is within this capacity, the resource is deemed satisfactory; otherwise, it will be in outage. Also, the user's required communication rate is established by the threshold γ. The OP of a single resource j is [9, eq. (4)]:

$$P_1\left(\gamma\right) \triangleq \mathbb{P}\left[C\left(H_j(t+l,l)\right) < \gamma\right] \quad \forall j \in \mathsf{R}. \quad (2)$$

The user utilizes an ML-based classifier for resource allocation. Here, resources are indexed using the set $\mathsf{R} = \{1, 2, \cdots, |\mathsf{R}|\}$, and resource $j \in \mathsf{R}$ is the jth resource being explored by the allocation procedure. If the ML model predicts an outage, j is incremented by 1. For each resource j, the model evaluates the current channel conditions $H_j(t, \mathtt{k})$, producing an output in $[0, 1]$. If this output is less than a classification threshold $\mathtt{q_{th}}$, the upcoming l channel samples, i.e., $H_j(t+l, l)$, are determined to support outage-free communication for each resource $j \in \mathsf{R}$. If no such resource is found, the model selects the final resource.

Specifically, $\mathsf{Q}\left(H_j(t,\mathtt{k});\Theta\right) \in [0,1]$, where Θ indicates the parameters for the model Q. If $\mathsf{Q}\left(H_j(t,\mathtt{k});\Theta\right) > \mathtt{q_{th}}$, an outage is predicted for the next l channel samples. The model's cumulative distribution function is [9, eq. (8)]:

$$F_{\mathsf{Q}}\left(x\right) \triangleq \mathbb{P}\left[\mathsf{Q}\left(H_j(t,\mathtt{k});\Theta\right) \le x\right] \quad \forall j \in \mathsf{R}. \quad (3)$$

The OP of a system with $|\mathsf{R}|$ resources is [9, eq. (13)]:

$$P_{|\mathsf{R}|}\left(\gamma,\mathtt{q_{th}}\right) = P_1\left(\gamma\right)\left(1-F_{\mathsf{Q}}\left(\mathtt{q_{th}}\right)\right)^{|\mathsf{R}|-1} + P_\infty\left(\gamma,\mathtt{q_{th}}\right)\left(1-\left(1-F_{\mathsf{Q}}\left(\mathtt{q_{th}}\right)\right)^{|\mathsf{R}|-1}\right), \quad (4)$$

where $P_\infty\left(\gamma,\mathtt{q_{th}}\right) \triangleq \lim_{|\mathsf{R}|\to\infty} P_{|\mathsf{R}|}\left(\gamma,\mathtt{q_{th}}\right)$

$$= \mathbb{P}\left[C(H_j(t+l,l)) < \gamma \,|\, \mathsf{Q}\left(H_j(t,\mathtt{k})\right) \le \mathtt{q_{th}}\right]. \quad (5)$$

The OLF for this system is given in [9, eq. (29)], and serves as an approximation to the OP in (4). Thus, minimizing the OLF, as shown in [9], effectively reduces the system's OP.

III. Optimal Classifier

This section outlines the necessary and sufficient conditions that an optimal classifier should satisfy.

Theorem 1. *The OP, $P_{|\mathsf{R}|}(\gamma,\mathtt{q_{th}})$ in (4), has a lower-bound of $P_1(\gamma)^{|\mathsf{R}|}$. This is achieved if and only if $F_{\mathsf{Q}}\left(\mathtt{q_{th}}\right) = 1 - P_1(\gamma)$ and $P_\infty(\gamma,\mathtt{q_{th}}) = 0$. If the predictor achieves $P_{|\mathsf{R}|}(\gamma,\mathtt{q_{th}}) = P_1(\gamma)^{|\mathsf{R}|}$, it is referred to as an optimal ML outage classifier.*

Proof: See Appendix A. ∎

Theorem 1 tells us how an optimal outage predictor should be internally configured and when our quest for a good predictor should stop. It also tells us that if we are given an optimal predictor then it must be true that $F_{\mathsf{Q}}\left(\mathtt{q_{th}}\right) = 1 - P_1(\gamma)$ and $P_\infty(\gamma,\mathtt{q_{th}}) = 0$. Conversely, if we are given a predictor and told that $F_{\mathsf{Q}}\left(\mathtt{q_{th}}\right) = 1 - P_1(\gamma)$ and $P_\infty(\gamma,\mathtt{q_{th}}) = 0$, then we immediately know that it is also optimal. Importantly, the condition $P_\infty(\gamma,\mathtt{q_{th}}) = 0$ suggests that the model and the channel are perfectly correlated, a situation that could only arise if the channel exhibits no decorrelation properties. This implies that the optimal performance can only be achieved in a perfectly correlated environment. Of course, the greater the correlation between the samples the better the performance. The optimal classifier establishes a non-trivial outage performance lower bound, indicating when our training is nearing a limit beyond which we know to be unachievable. This bound is independent of the neural network architecture. Thus if the performance nears this limit, further architectural changes are unnecessary, and our quest for a good predictor should stop.

IV. Mean Number of Scanned Resources

If the set of resources R is indexed from 1 to $|\mathsf{R}|$, on average, how many resources are scanned when identifying one that meets the required condition? Lemma 1 answers this.

Lemma 1. *Let $s \in \{1, \ldots, |\mathsf{R}|\}$ be the index of the resource selected by the user for transmission. Then*

$$\mathbb{E}\left[s\right] = \left(\frac{1-|\mathsf{R}|\left(1-F_{\mathsf{Q}}\left(\mathtt{q_{th}}\right)\right)^{|\mathsf{R}|-1}}{F_{\mathsf{Q}}\left(\mathtt{q_{th}}\right)}\right) + \left(\frac{\left(|\mathsf{R}|-1\right)\left(1-F_{\mathsf{Q}}\left(\mathtt{q_{th}}\right)\right)^{|\mathsf{R}|}}{F_{\mathsf{Q}}\left(\mathtt{q_{th}}\right)}\right) + |\mathsf{R}|\left(1-F_{\mathsf{Q}}\left(\mathtt{q_{th}}\right)\right)^{|\mathsf{R}|-1}. \quad (6)$$

It then follows that, for a one-resource allocation policy, the mean number of rejected resources is $\mathbb{E}\left[s\right] - 1$. Finally, as $|\mathsf{R}| \to \infty$, $\mathbb{E}\left[s\right] \to \frac{1}{F_{\mathsf{Q}}\left(\mathtt{q_{th}}\right)}$; as $F_{\mathsf{Q}}\left(\mathtt{q_{th}}\right) \to 0$, $\mathbb{E}\left[s\right] \to |\mathsf{R}|$; and as $F_{\mathsf{Q}}\left(\mathtt{q_{th}}\right) \to 1$, $\mathbb{E}\left[s\right] \to 1$.

Proof: See Appendix B. ∎

For fixed R, because the expected number of resources scanned depends only on $F_{\mathsf{Q}}\left(\mathtt{q_{th}}\right)$, by combining this lemma with Theorem 1, we can substitute $F_{\mathsf{Q}}\left(\mathtt{q_{th}}\right) = 1 - P_1\left(\gamma\right)$ in (6) to obtain the average number of scanned resources by the OpM. We exploit this observation in our results section. The limiting behaviors below (6) are fairly intuitive. For the first, as $|\mathsf{R}| \to \infty$, the resource selection index becomes geometrically distributed according to $\mathrm{Geo}\left(F_{\mathsf{Q}}(\mathtt{q_{th}})\right)$. The mean of such a distribution is $1/F_{\mathsf{Q}}(\mathtt{q_{th}})$. For the second, as the resource acceptance probability goes to 0, the system tends toward always selecting the final resource. Finally, for the third, as the resource acceptance probability goes to 1, the system tends toward always selecting the first resource.

V. Monte Carlo Simulations

A. Data Generation and Training

To generate $\mathtt{k}+l$ channel samples for each resource, we use the correlation model in [9, Section V]. This model introduces a uniformly distributed phase shift (parameterized by ξ, varied from 0.01 to 0.9) for each time increment. It was shown to align with Clarke's 3D model [11], which reflects mobility in a fading environment, and has an autocorrelation between successive channel samples proportional to $\mathrm{sinc}(\xi)$. Then, we employ a DQN-LSTM model, outlined in [12], leveraging both

TABLE I
PARAMETERS OF THE DQN-LSTM MODEL

Parameter	Value	Parameter	Value
Epochs	30	Learning rate	0.001
Epoch size	150	Discount factor	0.9
Hidden units	32	Input length ($\mathtt{k}$)	100
Epsilon	Decaying strategy	Output length (l)	10
Rewards	1 (correct prediction)	Output	1
	-1 (otherwise)	dimension	

the OLF with $\mathtt{q_{th}} = 0.1$ and 0.5, and $\alpha = 10$, as well as the BCE loss function. From Table I, the hyperparameters for training the DQN-LSTM model include $\mathtt{k} = 100$ and $l = 10$. We use the first $\mathtt{k}$ samples, $H_j(t, \mathtt{k})$, as input to the DQN-LSTM model. The subsequent l samples, $H_j(t + l, l)$, are used to generate a single label, indicating the system's ability to support communication over those l samples at a determined rate. The model then processes the next $\mathtt{k}$ samples that follow these l samples. The supporting code can be found here [13].

B. Results

Fig. 1(a) shows the OP of a 4-resource system using both the OpM and non-OpMs at $\gamma = 1.0$ and SNRs of 2 dB and 5 dB, across varying correlation values for $\mathtt{q_{th}} = 0.1$ and 0.5. As per Theorem 1, optimal performance is achieved when the model and channel are perfectly correlated. As this correlation $\to 1$, the performances of the OpM and non-OpMs converge; conversely, as the correlation $\to 0$ (i.e., $\xi \to \infty$), the performance disparity between these widens, with the predictive performance of non-OpMs aligning with the OP of a single resource system, i.e., $P_1(\gamma)$. We also note that $P_1(\gamma)$ increases with the increase of correlation. This is because correlation in a fading environment, as is well known, has a deleterious effect on diversity. On the other hand, with more (independent) resources available, this deleterious effect is offset and the OP of multi-resource systems declines.

From the same figure, for a fixed $\mathtt{q_{th}}$ and intermediate (practical) correlation values, OLF demonstrates better performance compared to BCE. Also, for the OLF, the OP negligibly changes with $\mathtt{q_{th}}$ because it is optimized for the specific $\mathtt{q_{th}}$ used for training. Minor discrepancies are due to variations in the training[1] procedure. However, the OP with BCE varies, as BCE does not depend on $\mathtt{q_{th}}$ during training, resulting in variable results across different values of $\mathtt{q_{th}}$ when testing. Fig. 1(b) shows the OP of a 4-resource system when using OpM and non-OpMs for $\mathtt{q_{th}} = 0.5$, $\gamma = 1.0$ across varying SNRs for decreasing ξ (or increasing correlation). The OP of the OpM versus SNR is also shown. In high SNR regions, we see that very small levels of decorrelation in the channel result in large performance gaps between non-OpMs and OpM.

Fig. 2(a) shows the average number of rejected resources for an 8-resource system with OpM and non-OpMs for $\mathtt{q_{th}} = 0.1$, $\gamma = 1.5$ and for a range of SNRs. Here, BCE consistently chooses the first resource when the SNR is high and the outages are infrequent. For the same $\mathtt{q_{th}}$, the OLF shows greater care

[1]Each data point in the figures represents the average performance obtained after independently retraining the ML model several times, leading to the expected discrepancies that tend to be mitigated through averaging.

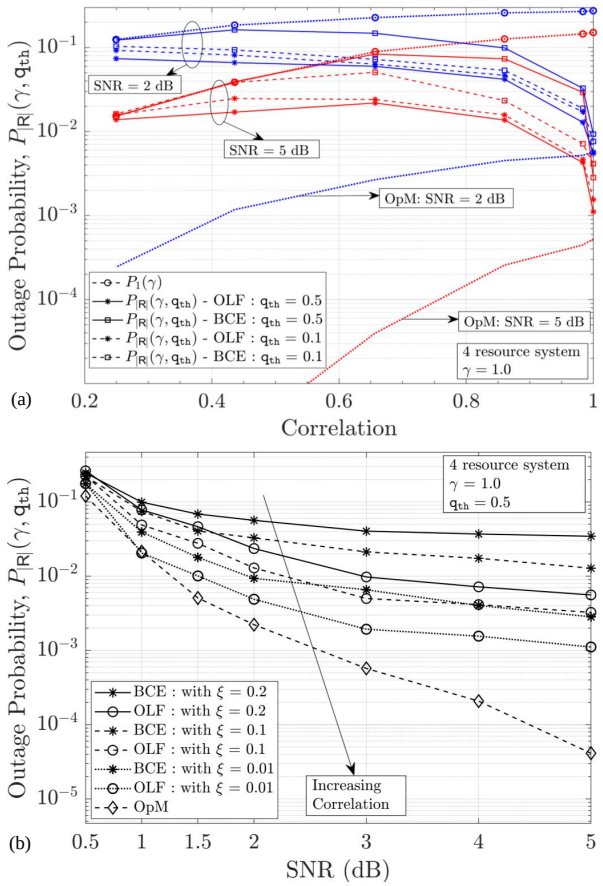

Fig. 1. Monte Carlo simulations for a 4-resource system. (a): $P_{|\mathtt{R}|}(\gamma, \mathtt{q_{th}})$ vs. correlation with BCE and outage losses, for $\mathtt{q_{th}} = 0.1$ and 0.5, at 2 dB and 5 dB, including OP of OpM and $P_1(\gamma)$. (b): $P_{|\mathtt{R}|}(\gamma, \mathtt{q_{th}})$ vs. SNR with BCE and outage losses, including OP of OpM, for decreasing phase shifts.

when accepting resources (it learns not to always accept the first resource). Also, models trained with both loss functions do not reject a vastly different number of resources than the OpM. Note that rejecting a similar amount of resources as the OpM is not necessarily good. Indeed, it can be achieved trivially using a no-skill model that simply rejects resources with a probability equal to the resource OP. The OP plot for an 8-resource system is shown in Fig. 2(b). It is evident that while the OLF results in a slight increase in the average number of rejected resources, it significantly enhances the probability of minimizing system outages. For example, at SNR = 5 dB, OLF rejected approximately 64% more resources than BCE, leading to a decrease in OP by approximately 93% relative to BCE. In absolute figures, the difference in performance between the two algorithms, favoring OLF, is more noticeable. While the average number of rejected resources is similar for both (0.30 for BCE and 0.49 for OLF), the OP of OLF (2×10^{-4}) is improved by one order of magnitude compared to BCE (3×10^{-3}). In practice, this may mean meeting (OLF) or not meeting (BCE) the operational requirement.

VI. CONCLUSIONS AND FUTURE WORK

This paper determined the necessary and sufficient conditions for an optimal outage classifier in an ML-assisted resource allocation system introduced in [9]. We showed that

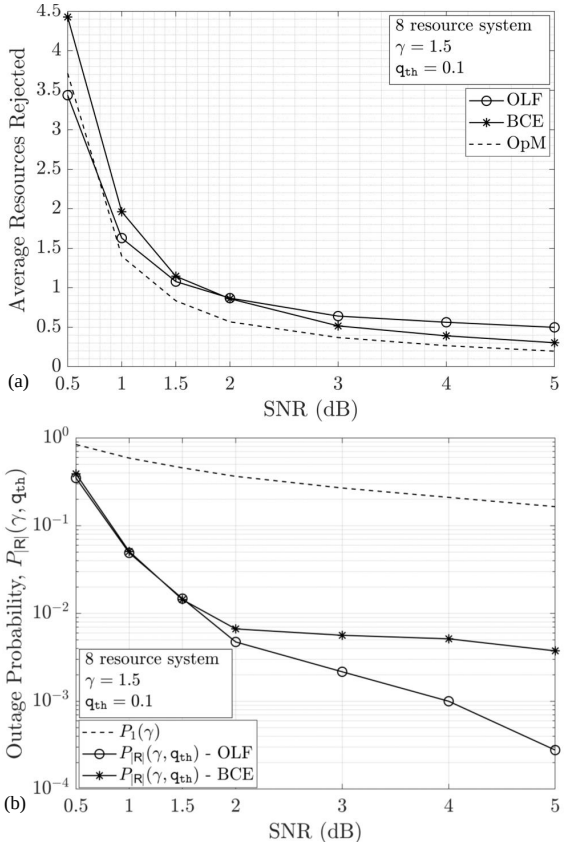

Fig. 2. Monte Carlo simulations for an 8-resource system. (a): average resources rejected vs. SNR with BCE and OLF, including that rejected by the OpM. (b): $P_{|\mathsf{R}|}(\gamma, \mathtt{q_{th}})$ vs. SNR with BCE and OLF, including $P_1(\gamma)$.

optimal performance requires channels without time decorrelation. Utilizing a DQN methodology, we assessed various correlation scenarios. Observations revealed that OLF and BCE-trained models approached OpM performance as correlation neared unity, while at intermediate (practical) correlation values, OLF-trained models outperformed BCE-trained ones. Lastly, we illustrated the trade-off between enhancing outage performance and an increase in the mean number of rejected resources, with OLF surpassing BCE in outage performance for identical $\mathtt{q_{th}}$. Future work will focus on establishing achievable lower OP bounds for arbitrary correlation levels of the system, and extending these to multi-user scenarios.

APPENDIX

A. Proof of Theorem 1

We consider the proof of this theorem in three parts:

1) We first prove that $P_{|\mathsf{R}|}(\gamma, \mathtt{q_{th}}) \geq P_1(\gamma)^{|\mathsf{R}|}$.
2) We then prove that if $(1 - F_{\mathsf{Q}}(\mathtt{q_{th}})) = P_1(\gamma)$ and $P_\infty(\gamma, \mathtt{q_{th}}) = 0$, we must have $P_{|\mathsf{R}|}(\gamma, \mathtt{q_{th}}) = P_1(\gamma)^{|\mathsf{R}|}$.
3) Finally, we prove that if $P_{|\mathsf{R}|}(\gamma, \mathtt{q_{th}}) = P_1(\gamma)^{|\mathsf{R}|}$ we must have $(1 - F_{\mathsf{Q}}(\mathtt{q_{th}})) = P_1(\gamma)$ and $P_\infty(\gamma, \mathtt{q_{th}}) = 0$.

This will complete the proof. Items 1 and 2 above follow immediately from the second part of Lemma 2:

- Clearly the lower bound of (10) is greater than $P_1(\gamma)^{|\mathsf{R}|}$.
- Clearly, substituting $F_{\mathsf{Q}}(\mathtt{q_{th}}) = 1 - P_1(\gamma)$ and $P_\infty(\gamma, \mathtt{q_{th}}) = 0$ into (10) results in a squeezing effect: the upper and lower bounds equal each other, forcing $P_{|\mathsf{R}|}(\gamma, \mathtt{q_{th}}) = P_1(\gamma)^{|\mathsf{R}|}$. Note, this could have also been shown through direct substitutions into (4).

To prove item 3, assume $P_{|\mathsf{R}|}(\gamma, \mathtt{q_{th}}) = P_1(\gamma)^{|\mathsf{R}|}$. We now show that this implies $P_\infty(\gamma, \mathtt{q_{th}}) = 0$:

$$P_\infty(\gamma, \mathtt{q_{th}}) = \lim_{|\mathsf{R}|\to\infty} P_{|\mathsf{R}|}(\gamma, \mathtt{q_{th}}) = \lim_{|\mathsf{R}|\to\infty} P_1(\gamma)^{|\mathsf{R}|} = 0,$$

where the first equality follows from (5), the second follows from our assumption immediately above, and the third follows from the assumption that $0 < P_1(\gamma) < 1$. This goes part way to proving item 3. Finally, we show that the assumption $P_{|\mathsf{R}|}(\gamma, \mathtt{q_{th}}) = P_1(\gamma)^{|\mathsf{R}|}$ implies that $F_{\mathsf{Q}}(\mathtt{q_{th}}) = 1 - P_1(\gamma)$:

$$\begin{aligned} P_{|\mathsf{R}|}(\gamma, \mathtt{q_{th}}) &= P_1(\gamma)^{|\mathsf{R}|} \\ &\implies \max\Big\{P_1(\gamma)^{|\mathsf{R}|}, \\ &\quad (1 - F_{\mathsf{Q}}(\mathtt{q_{th}}))^{|\mathsf{R}|-1} P_1(\gamma)\Big\} \leq P_1(\gamma)^{|\mathsf{R}|} \qquad (7) \\ &\implies \max\left\{1, \frac{(1 - F_{\mathsf{Q}}(\mathtt{q_{th}}))^{|\mathsf{R}|-1}}{P_1(\gamma)^{|\mathsf{R}|-1}}\right\} \leq 1 \\ &\implies \frac{1 - F_{\mathsf{Q}}(\mathtt{q_{th}})}{P_1(\gamma)} \leq 1 \\ &\Downarrow \qquad\qquad \text{or} \qquad\qquad \Downarrow \\ 1 - F_{\mathsf{Q}}(\mathtt{q_{th}}) &< P_1(\gamma) \qquad 1 - F_{\mathsf{Q}}(\mathtt{q_{th}}) = P_1(\gamma) \\ &\Downarrow \qquad\qquad\qquad\quad \Downarrow \\ P_\infty(\gamma, \mathtt{q_{th}}) &> 0 \qquad\qquad P_\infty(\gamma, \mathtt{q_{th}}) \geq 0 \end{aligned} \qquad (8)$$

where (7) follows from the second part of Lemma 2 and (8) follows from the first part of Lemma 2. But $P_\infty(\gamma, \mathtt{q_{th}}) > 0$ contradicts our proof above that $P_\infty(\gamma, \mathtt{q_{th}}) = 0$ for $P_{|\mathsf{R}|}(\gamma, \mathtt{q_{th}}) = P_1(\gamma)^{|\mathsf{R}|}$. Therefore, $1 - F_{\mathsf{Q}}(\mathtt{q_{th}}) < P_1(\gamma)$ is not possible[2] and (8) reduces to just $1 - F_{\mathsf{Q}}(\mathtt{q_{th}}) = P_1(\gamma) \implies P_\infty(\gamma, \mathtt{q_{th}}) \geq 0$. This completes the proof.

Lemma 2. *Consider $F_{\mathsf{Q}}(\mathtt{q_{th}})$ given in (3) and $P_\infty(\gamma, \mathtt{q_{th}})$ in (5). Then the following two statements hold.*

1) $F_{\mathsf{Q}}(\mathtt{q_{th}})$ and $P_\infty(\gamma, \mathtt{q_{th}})$ satisfy the following bound

$$P_\infty(\gamma, \mathtt{q_{th}}) \geq \frac{P_1(\gamma) - 1 + F_{\mathsf{Q}}(\mathtt{q_{th}})}{F_{\mathsf{Q}}(\mathtt{q_{th}})}. \qquad (9)$$

Consequently, as the probability of resource allocation goes to 1 (i.e., $F_{\mathsf{Q}}(\mathtt{q_{th}}) \to 1$), we have $P_\infty(\gamma, \mathtt{q_{th}}) \geq P_1(\gamma)$; and for $P_\infty(\gamma, \mathtt{q_{th}}) \to 0$, the probability of resource allocation satisfies $F_{\mathsf{Q}}(\mathtt{q_{th}}) \leq 1 - P_1(\gamma)$.

2) The system's OP in (4) satisfies the following bound:

$$\begin{aligned} &\max\Big\{P_1(\gamma)^{|\mathsf{R}|}, (1 - F_{\mathsf{Q}}(\mathtt{q_{th}}))^{|\mathsf{R}|-1} P_1(\gamma)\Big\} \leq P_{|\mathsf{R}|}(\gamma, \mathtt{q_{th}}) \\ &\leq \Big(P_\infty(\gamma, \mathtt{q_{th}}) + P_1(\gamma)(1 - F_{\mathsf{Q}}(\mathtt{q_{th}}))^{|\mathsf{R}|-1}\Big). \qquad (10) \end{aligned}$$

Proof: For brevity, let $C := C(H_j(t+l, l))$ and $\mathsf{Q} := \mathsf{Q}(H_j(t, \mathtt{k}))$. We now prove the first part of the lemma:

$$\begin{aligned} P_\infty(\gamma, \mathtt{q_{th}}) &= \mathbb{P}[C < \gamma \mid \mathsf{Q} \leq \mathtt{q_{th}}] \qquad (11) \\ &= \frac{\mathbb{P}[\mathsf{Q} \leq \mathtt{q_{th}} \mid C < \gamma] P_1(\gamma)}{F_{\mathsf{Q}}(\mathtt{q_{th}})} \qquad (12) \\ &= \frac{\mathbb{P}[\mathsf{Q} \leq \mathtt{q_{th}} \cap C < \gamma]}{F_{\mathsf{Q}}(\mathtt{q_{th}})} \qquad (13) \end{aligned}$$

[2]Meaning we can ignore the implications to the left-hand-side of the "or".

$$= \frac{1-\mathbb{P}\left[\mathsf{Q} > \mathsf{q}_{\mathtt{th}} \cup C \geq \gamma\right]}{F_{\mathsf{Q}}\left(\mathsf{q}_{\mathtt{th}}\right)} \tag{14}$$

$$= \frac{1-\mathbb{P}\left[C \geq \gamma\right] - \mathbb{P}\left[\mathsf{Q} > \mathsf{q}_{\mathtt{th}}\right]}{F_{\mathsf{Q}}\left(\mathsf{q}_{\mathtt{th}}\right)} + \frac{\mathbb{P}\left[\mathsf{Q} > \mathsf{q}_{\mathtt{th}} \cap C \geq \gamma\right]}{F_{\mathsf{Q}}\left(\mathsf{q}_{\mathtt{th}}\right)} \tag{15}$$

$$= \frac{P_1(\gamma) - 1 + F_{\mathsf{Q}}\left(\mathsf{q}_{\mathtt{th}}\right)}{F_{\mathsf{Q}}\left(\mathsf{q}_{\mathtt{th}}\right)} + \frac{\mathbb{P}\left[\mathsf{Q} > \mathsf{q}_{\mathtt{th}} \cap C \geq \gamma\right]}{F_{\mathsf{Q}}\left(\mathsf{q}_{\mathtt{th}}\right)} \tag{16}$$

$$\geq \frac{P_1(\gamma) - 1 + F_{\mathsf{Q}}\left(\mathsf{q}_{\mathtt{th}}\right)}{F_{\mathsf{Q}}\left(\mathsf{q}_{\mathtt{th}}\right)} \tag{17}$$

where (12) and (13) follow from an application of Bayes' theorem, (14) is from de Morgan's law [14], (15) is a consequence of the addition law of probabilities, and (16) is from $\mathbb{P}\left[C \geq \gamma\right] = 1 - P_1(\gamma)$ and the definition of $F_{\mathsf{Q}}\left(\mathsf{q}_{\mathtt{th}}\right)$. For the second part of the lemma, we consider the upper and lower bounds separately. For the upper bound, from (4) we have

$$\begin{aligned} P_{|\mathsf{R}|}(\gamma, \mathsf{q}_{\mathtt{th}}) &= P_{\infty}(\gamma, \mathsf{q}_{\mathtt{th}}) \left(1 - \left(1 - F_{\mathsf{Q}}\left(\mathsf{q}_{\mathtt{th}}\right)\right)^{|\mathsf{R}|-1}\right) \\ &\quad + P_1\left(\gamma\right)\left(1 - F_{\mathsf{Q}}\left(\mathsf{q}_{\mathtt{th}}\right)\right)^{|\mathsf{R}|-1} \\ &= P_{\infty}(\gamma, \mathsf{q}_{\mathtt{th}}) - P_{\infty}\left(\gamma, \mathsf{q}_{\mathtt{th}}\right) \\ &\quad \times \left(1 - F_{\mathsf{Q}}\left(\mathsf{q}_{\mathtt{th}}\right)\right)^{|\mathsf{R}|-1} + P_1\left(\gamma\right) \\ &\quad \times \left(1 - F_{\mathsf{Q}}\left(\mathsf{q}_{\mathtt{th}}\right)\right)^{|\mathsf{R}|-1} \qquad (18) \\ &\leq P_{\infty}(\gamma, \mathsf{q}_{\mathtt{th}}) + P_1\left(\gamma\right)\left(1 - F_{\mathsf{Q}}\left(\mathsf{q}_{\mathtt{th}}\right)\right)^{|\mathsf{R}|-1}. \qquad (19) \end{aligned}$$

For the lower bound, we first prove $P_{|\mathsf{R}|}(\gamma, \mathsf{q}_{\mathtt{th}}) \geq P_1(\gamma)^{|\mathsf{R}|}$. Then, we prove $P_{|\mathsf{R}|}(\gamma, \mathsf{q}_{\mathtt{th}}) \geq P_1\left(\gamma\right)\left(1 - F_{\mathsf{Q}}\left(\mathsf{q}_{\mathtt{th}}\right)\right)^{|\mathsf{R}|-1}$. To prove $P_{|\mathsf{R}|}(\gamma, \mathsf{q}_{\mathtt{th}}) \geq P_1(\gamma)^{|\mathsf{R}|}$, note that a system outage for the user will necessarily occur if *all* resources are in outage. System outages may also occur if good resources were rejected in favour of a bad resource. So system outages must be at least as probable as all resources being in outage. Because all the resources are i.i.d., the probability that all the resources are in outage is $P_1(\gamma)^{|\mathsf{R}|}$. This proves $P_{|\mathsf{R}|}(\gamma, \mathsf{q}_{\mathtt{th}}) \geq P_1(\gamma)^{|\mathsf{R}|}$. To prove $P_{|\mathsf{R}|}(\gamma, \mathsf{q}_{\mathtt{th}}) \geq P_1\left(\gamma\right)\left(1 - F_{\mathsf{Q}}\left(\mathsf{q}_{\mathtt{th}}\right)\right)^{|\mathsf{R}|-1}$, from (4):

$$\begin{aligned} P_{|\mathsf{R}|}\left(\gamma, \mathsf{q}_{\mathtt{th}}\right) &= P_{\infty}\left(\gamma, \mathsf{q}_{\mathtt{th}}\right) \left(1 - \left(1 - F_{\mathsf{Q}}\left(\mathsf{q}_{\mathtt{th}}\right)\right)^{|\mathsf{R}|-1}\right) \\ &\quad + P_1\left(\gamma\right)\left(1 - F_{\mathsf{Q}}\left(\mathsf{q}_{\mathtt{th}}\right)\right)^{|\mathsf{R}|-1} \\ &\geq P_1\left(\gamma\right)\left(1 - F_{\mathsf{Q}}\left(\mathsf{q}_{\mathtt{th}}\right)\right)^{|\mathsf{R}|-1} \qquad (20) \end{aligned}$$

where (20) follows because the term $P_{\infty}(\gamma, \mathsf{q}_{\mathtt{th}}) \left(1 - \left(1 - F_{\mathsf{Q}}\left(\mathsf{q}_{\mathtt{th}}\right)\right)^{|\mathsf{R}|-1}\right)$ is always non-negative (since $F_{\mathsf{Q}}\left(\mathsf{q}_{\mathtt{th}}\right)$ and $P_{\infty}(\gamma, \mathsf{q}_{\mathtt{th}})$ are probabilities, i.e., $0 \leq F_{\mathsf{Q}}\left(\mathsf{q}_{\mathtt{th}}\right), P_{\infty}\left(\gamma, \mathsf{q}_{\mathtt{th}}\right) \leq 1$). This proves the lemma. ■

B. Proof of Lemma 1

$$\begin{aligned} \mathbb{E}\left[s\right] &\triangleq \sum_{j=1}^{|\mathsf{R}|} \mathbb{P}\left[s = j\right] j \qquad (21) \\ &= \sum_{j=1}^{|\mathsf{R}|-1} \left(1 - F_{\mathsf{Q}}\left(\mathsf{q}_{\mathtt{th}}\right)\right)^{j-1} \left(F_{\mathsf{Q}}\left(\mathsf{q}_{\mathtt{th}}\right)\right) j \\ &\quad + |\mathsf{R}| \left(1 - F_{\mathsf{Q}}\left(\mathsf{q}_{\mathtt{th}}\right)\right)^{|\mathsf{R}|-1} \qquad (22) \\ &= \left(\frac{1 - |\mathsf{R}| \left(1 - F_{\mathsf{Q}}\left(\mathsf{q}_{\mathtt{th}}\right)\right)^{|\mathsf{R}|-1}}{F_{\mathsf{Q}}\left(\mathsf{q}_{\mathtt{th}}\right)}\right) \\ &\quad + \left(\frac{\left(|\mathsf{R}| - 1\right)\left(1 - F_{\mathsf{Q}}\left(\mathsf{q}_{\mathtt{th}}\right)\right)^{|\mathsf{R}|}}{F_{\mathsf{Q}}\left(\mathsf{q}_{\mathtt{th}}\right)}\right) \\ &\quad + |\mathsf{R}| \left(1 - F_{\mathsf{Q}}\left(\mathsf{q}_{\mathtt{th}}\right)\right)^{|\mathsf{R}|-1}, \qquad (23) \end{aligned}$$

where (21) follows from the definition of expectation and (22) follows after noting that $1 - F_{\mathsf{Q}}\left(\mathsf{q}_{\mathtt{th}}\right)$ is the probability of resource rejection, so for $j < |\mathsf{R}|$, $\mathbb{P}\left[s = j\right]$ is equal to the probability that $j - 1$ resources have been rejected, i.e., $\left(1 - F_{\mathsf{Q}}\left(\mathsf{q}_{\mathtt{th}}\right)\right)^{j-1}$, multiplied by the probability that the jth resource is selected, i.e., $F_{\mathsf{Q}}\left(\mathsf{q}_{\mathtt{th}}\right)$. When $j = |\mathsf{R}|$, the resource is always selected if all resources before it were rejected, so $\mathbb{P}\left[s = |\mathsf{R}|\right] = \left(1 - F_{\mathsf{Q}}\left(\mathsf{q}_{\mathtt{th}}\right)\right)^{|\mathsf{R}|-1}$. Finally, (23) follows from the known solution to power sums [15].

REFERENCES

[1] H. Yang, A. Alphones, Z. Xiong, D. Niyato, J. Zhao, and K. Wu, "Artificial-Intelligence-Enabled Intelligent 6G Networks," *IEEE Netw.*, vol. 34, no. 6, pp. 272–280, Oct. 2020.

[2] A. Alkhateeb, I. Beltagy, and S. Alex, "Machine Learning for Reliable mmWave Systems: Blockage Prediction and Proactive Handoff," in *2018 IEEE Global Conf. on Signal and Inf. Process. (GlobalSIP)*, Anaheim, CA, Feb. 2018, pp. 1055–1059.

[3] H. Sarieddeen, N. Saeed, T. Y. Al-Naffouri, and M.-S. Alouini, "Next Generation Terahertz Communications: A Rendezvous of Sensing, Imaging, and Localization," *IEEE Commun. Mag.*, vol. 58, no. 5, pp. 69–75, May 2020.

[4] L. Sanguinetti, A. Zappone, and M. Debbah, "Deep Learning Power Allocation in Massive MIMO," in *52nd Asilomar Conf. on Signals, Syst., and Comp.*, Pacific Grove, CA, USA, Oct. 2018, pp. 1257–1261.

[5] H. Ye, G. Y. Li, and B.-H. F. Juang, "Deep Reinforcement Learning based Resource Allocation for V2V Communications," *IEEE Trans. on Veh. Technol.*, vol. 68, no. 4, pp. 3163–3173, April 2019.

[6] C. She, C. Sun, Z. Gu, Y. Li, C. Yang, H. V. Poor, and B. Vucetic, "A Tutorial on Ultrareliable and Low-latency Communications in 6G: Integrating Domain Knowledge Into Deep Learning," *Proc. of the IEEE*, vol. 109, no. 3, pp. 204–246, March 2021.

[7] K. Utkarsh, Ashish, and P. Kumar, "Transmit Power Reduction in an IRS Aided Wireless Communication System using DNN," in *2023 Int. Conf. on Microw., Opt., and Commun. Eng. (ICMOCE)*, Bhubaneswar, India, May 2023, pp. 1–5.

[8] H. Chergui, L. Blanco, and C. Verikoukis, "Statistical Federated Learning for Beyond 5G SLA-Constrained RAN Slicing," *IEEE Trans. on Wireless Commun.*, vol. 21, no. 3, pp. 2066–2076, Sept. 2022.

[9] N. Simmons, D. E. Simmons, and M. D. Yacoub, "Outage Performance and Novel Loss Function for an ML-Assisted Resource Allocation: An Exact Analytical Framework," *IEEE Trans. on Mach. Learn. in Commun. and Netw.*, vol. 2, pp. 335–350, Feb. 2024.

[10] D. Tse and P. Viswanath, *Fundamentals of Wireless Communication*. USA: Cambridge University Press, 2005.

[11] R. Clarke and W. L. Khoo, "3-D Mobile Radio Channel Statistics," *IEEE Trans. on Veh. Technol.*, vol. 46, no. 3, pp. 798–799, Aug. 1997.

[12] R. Raina, N. Simmons, D. E. Simmons, and M. D. Yacoub, "ML-Assisted Resource Allocation Outage Probability: Simple, Closed-Form Approximations," in *2023 IEEE Int. Conf. on Adv. Netw. and Telecommun. Syst. (ANTS)*, Jaipur, India, Dec. 2023, pp. 1–6.

[13] "Code for ML-Assisted Resource Allocation Outage Probability: Simple, Closed-Form Approximations," Nov. 2023, https://github.com/ML4Comms/greedy-resource-allocation-outage-classification.

[14] E. W. Weisstein, "De Morgan's Laws." MathWorld–A Wolfram Web Resource. [Online]. Available: https://mathworld.wolfram.com/deMorgansLaws.html

[15] ——, "Power Sum." MathWorld–A Wolfram Web Resource. [Online]. Available: https://mathworld.wolfram.com/PowerSum.html